Journal of Alloys and Compounds 499 (2010) 17–22

Contents lists available at ScienceDirect

Journal of Alloys and Compounds

journal homepage: www.elsevier.com/locate/jallcom

EPR and optical absorption studies of Cu^{2+} ions doped magnesium citrate decahydrate single crystals

Prashant Dwivedi [a,*], Ram Kripal [b,*], Madan Gopal Misra [b]

[a] Department of Physics, Kali Charan Nigam Institute of Technology, Banda (U.P.) 210001, India
[b] EPR Laboratory, Department of Physics, University of Allahabad, 22/5A Katra Road, Allahabad, 211002, India

ARTICLE INFO

Article history:
Received 28 December 2009
Received in revised form 11 March 2010
Accepted 12 March 2010
Available online 18 March 2010

PACS:
76.30

Keywords:
Organic crystals
Crystal growth
Crystal and ligand fields
Optical properties
Electron paramagnetic resonance

ABSTRACT

X-band electron paramagnetic resonance (EPR) studies of Cu^{2+} ions in magnesium citrate decahydrate single crystals are done at room temperature. Detailed EPR analysis indicates the presence of only one Cu^{2+} site. Cu^{2+} is found to take up substitutional position at Mg site. The angular variation of the EPR spectra in three planes a^*b, bc and ca^* are used to determine principal g and A tensors. The spin Hamiltonian parameters are: $g_x = 2.0346$, $g_y = 2.1400$, $g_z = 2.3874$, $A_x = 57$, $A_y = 76$, $A_z = 99$ ($\times 10^{-4}$) cm^{-1}. The optical absorption study is also carried out at room temperature and absorption bands are assigned to various transitions. The theoretical band positions are estimated using energy expressions and a good agreement is obtained with the experimental values. By correlating EPR and optical data, different molecular orbital coefficients are evaluated and the nature of bonding in the complex is discussed.

1. Introduction

EPR study enables to understand the symmetry of the electric field produced by the ligands around the metal ion [1–7]. It also provides a detailed description of the ground state of paramagnetic ion. The optical absorption study gives energy level structure of the metal ion. Thus, EPR and optical absorption yield crystal field symmetry around the metal ion and the nature of bonding between the metal ion and its various ligands. Citrates have many biological and medical applications [8,9] and thus any information obtained about their growth and characterizations are very useful. In the systematic study on the growth and characterization of several citrates, use has been made of EPR as one of the tools. Magnesium citrate is used to treat constipation. It is a hyperosmotic saline laxative. It pulls water from the tissues into the small intestines. The movement of water stimulates the normal forward movement of the intestines. It can cause certain medicines to not work as well like blood thinners, etc. [10]. If one is taking opioid, he will need to take laxatives regularly to counter their action on the bowel. Magnesium citrate helps relax muscles and aids in fighting depression. It is essential for the maintenance of ribonucleic acid (RNA) and deoxyribonucleic acid (DNA). It promotes cardiovascular health, works with vitamin B6 in alleviating premenstrual syndrome (PMS) and aids in tissue respiration [11]. It is also used to treat asthma and emphysema, attention deficit/hyperactivity disorder, type 2 diabetes, fibromyalgia, high blood pressure, human immunodeficiency virus (HIV), infertility and miscarriage, menopause, migraine headache, osteoporosis, etc. [12]. Urinary calcium excretion is reduced significantly by magnesium citrate in animals fed on high-calcium diets [9]. Significant advances have been made recently in the field of non-linear optics in the area of optoelectronic device technologies. Organic materials are quite relevant in this context because the delocalized electronic structure of π-bonded organic compound provides a number of opportunities in applications as non-linear optical materials [13]. Numerous uses of magnesium citrate mentioned above indicate that the synthesis and characterization of such a compound will be of immense importance. EPR studies of Cu^{2+} ion in sodium citrate [6], vanadyl ion in trisodium citrate [14] as well as triammonium citrate [15] were reported earlier. The present study deals with the results of EPR and optical absorption of Cu^{2+} ions doped in magnesium citrate decahydrate (MCD) single crystal at room temperature. The purpose of the study is to find the spin Hamiltonian parameters, crystal field symmetry and energy level structure of the metal ion and nature of bonding of the metal ion with different ligands that provides information about its technical application.

* Corresponding authors. Tel.: +91 532 2470532; fax: +91 532 2460993.
E-mail addresses: prashant_kcnit@rediffmail.com (P. Dwivedi), ram_kripal2001@rediffmail.com (R. Kripal).

0925-8388/$ – see front matter © 2010 Elsevier B.V. All rights reserved.
doi:10.1016/j.jallcom.2010.03.126

2. Crystal structure

The crystal structure of MCD was studied by Johnson [16]. The crystals are monoclinic and belong to space group $P2_1/n$. The unit cell dimensions are $a = 20.222$ Å, $b = 6.686$ Å and $c = 9.135$ Å and $\beta = 96.86^\circ$. The unit cell contains two $[Mg(H_2O)_6]^{2+}$ ions and four units of $[MgC_6H_5O_7(H_2O)]_2^- \cdot 2H_2O$. Each magnesium ion is coordinated to six oxygen atoms and there are no shared edges or corners between the two coordination octahedra. The magnesium at the center of symmetry, Mg (1), is a completely hydrated cation $[Mg(H_2O)_6]^{2+}$ and does not coordinate with the citrate oxygen atoms. The citrate ion is chelated to Mg (2) in a tridentate manner with the hydroxyl oxygen atom O (7) and two carboxyl oxygen atoms, one [O (4)] from an end carboxyl and one [O (5)] from the central carboxyl, forming the three points of attachment. The remaining three oxygen atoms of the second octahedron are a water oxygen atom [O (8)] and two carboxyl oxygen atoms [O (2′) and O (1″)] of two other citrate ions. These are related to the first by a b-lattice translation and by a two-fold screw operation, respectively. Only one water molecule [O (12)] is not coordinated to a magnesium.

3. Experimental

Single crystals of MCD, $[Mg(H_2O)_6][MgC_6H_5O_7\ (H_2O)]_2 \cdot 2H_2O$ were grown by slow evaporation of the saturated aqueous solution. The Cu^{2+} impurity was added by mixing 0.01 mole% of cupric chloride to the solution. After a few days, good single crystals of Cu^{2+} doped magnesium citrate decahydrate with well-developed faces were obtained. EPR spectra were recorded on X-band Varian E-4 spectrometer with 100 kHz field modulation at room temperature. A Varian flux meter with proton probe having 0.2 cm^3 of 0.25 M solution of $GdCl_3$ in H_2O was used for magnetic field measurement along with a Hewlett-Packard frequency counter . The measurement of EPR spectra are carried out by rotating the crystal about the three mutually perpendicular axes a^*, b and c in steps of 10°. The optical absorption spectra were recorded on a Unicam 5625-UV/vis spectrophotometer at room temperature in the wavelength range 195–325 and 325–1100 nm.

4. Results and discussion

The EPR spectra of Cu^{2+} doped MCD consist of four hyperfine lines as shown in Fig. 1. As given in the crystal structure, the unit cell contains two molecules per unit cell and hence two sets of four hyperfine lines should be observed. The observation of only one set

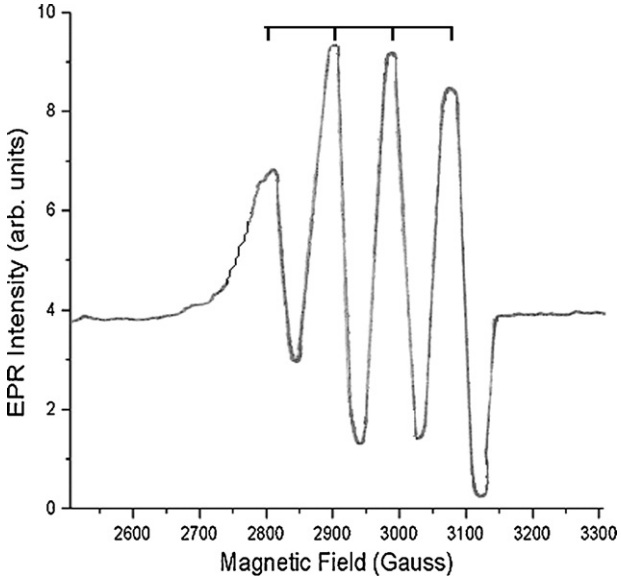

Fig. 1. EPR spectra of Cu^{2+} doped in magnesium citrate decahydrate when magnetic field is along a^* axis.

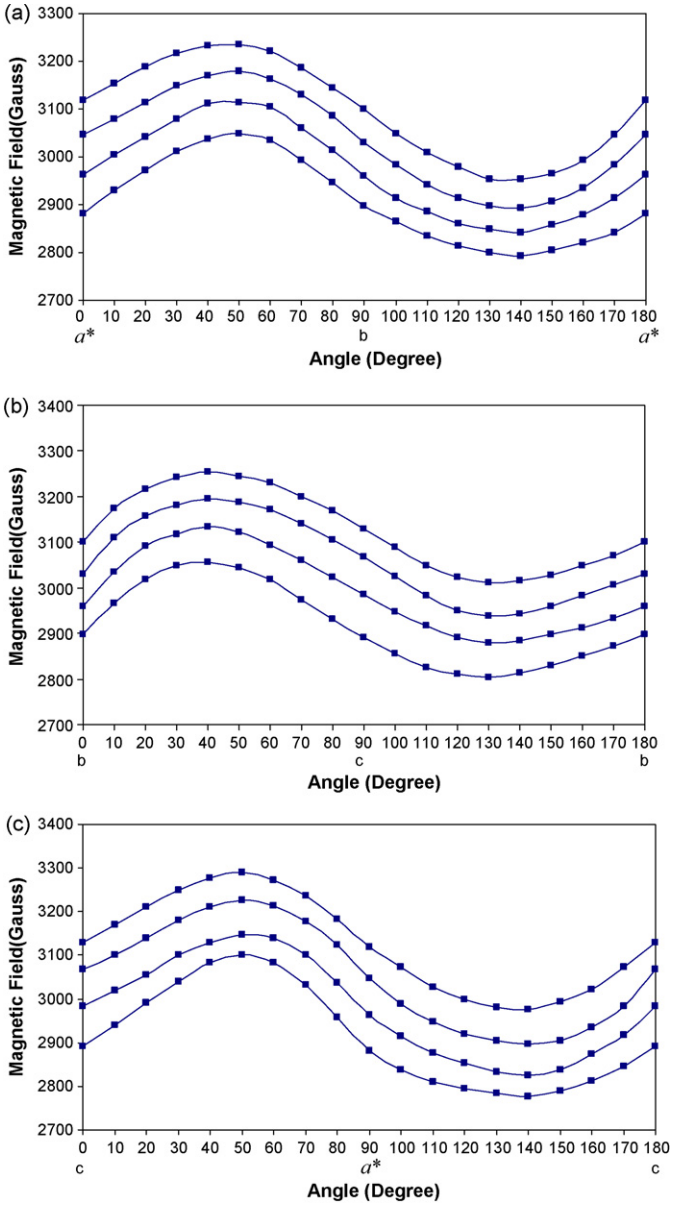

Fig. 2. (a) Angular variation of EPR spectra of Cu^{2+} ion in magnesium citrate decahydrate crystal for rotation in a^*b plane. (b) Angular variation of EPR spectra of Cu^{2+} ion in magnesium citrate decahydrate crystal for rotation in bc plane. (c) Angular Variation of EPR spectra of Cu^{2+} ion in magnesium citrate decahydrate crystal for rotation in ca^* plane.

of four hyperfine lines, thus indicates the presence of single Cu^{2+} ($S = 1/2$, $I = 3/2$) site in the lattice. Fig. 2(a–c) shows the variation of hyperfine lines in the three planes a^*b, bc and ca^*, respectively. The angular variation plots of g^2 (Fig. 3) indicate a rhombic local electric field symmetry for Cu^{2+} in MCD lattice. From the angular variation of the hyperfine pattern upon rotation about the a^*, b and c axis the principal values of g and A tensors for Cu^{2+} in MCD were evaluated by Schonland procedure [17] with the spin Hamiltonian:

$$H = \mu_B B_g S + S.A.I \quad (1)$$

The evaluated spin Hamiltonian parameters are given in Table 1. The values of these parameters of Cu^{2+} are similar to the results of earlier workers [18,19].

The Cu^{2+} ion can enter the lattice as a substitutional impurity in place of Mg. Therefore, the coordinating oxygens must determine the local electric field symmetry around the guest ion. A closer

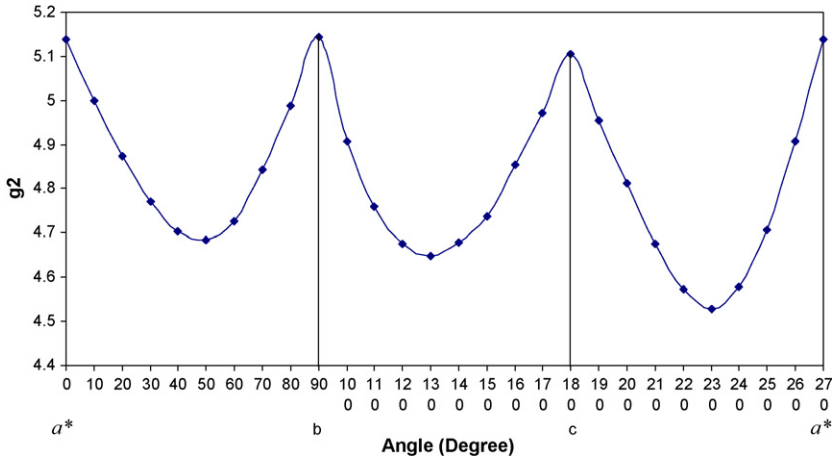

Fig. 3. Angular variation of the g^2 values of Cu^{2+} doped in magnesium citrate decahydrate crystal for rotation in a^*b, bc and ca^* planes.

Table 1
Principal g and A values and their direction cosines of Cu^{2+} in magnesium citrate decahydrate.

Principal g values	Direction cosines in a^*, b, c axis system			Principal A values ($10^{-4}cm^{-1}$)	Direction cosines in a^*, b, c axis system		
	a^*	b	c		a^*	b	c
2.0346	−0.3817	0.6577	−0.6494	57	0.0692	−0.8934	0.4439
2.1400	0.6107	−0.3480	−0.7113	76	0.1357	−0.4324	−0.8914
2.3874	0.6938	0.6681	0.2688	99	0.9883	0.1219	0.0913

Estimated errors for g and A values are ±0.0002 and $\pm 2 \times 10^{-4}$ cm^{-1}, respectively.

examination of the MCD crystal structure [16] shows that the unit cell is monoclinic and accommodates two molecules.

In MCD the cation exhibits six-fold coordination. The coordination polyhedra are distorted octahedra as shown in Fig. 4. The distorted octahedra around the Mg atom are inequivalent from the point of view of the Mg–O distances. Thus, they provide ideal sites for the Cu^{2+} ion imparting rhombic symmetry for the immediate environment of Cu^{2+}. The calculations as given in Table 2 show that the direction cosines of the Mg (2)–O (7) vector agree, with in experimental error, with those of g_z. This confirms that the Cu^{2+} ion has entered the lattice substitutionally in place of one of the two magnesium sites, Mg (2). The other direction cosines of the

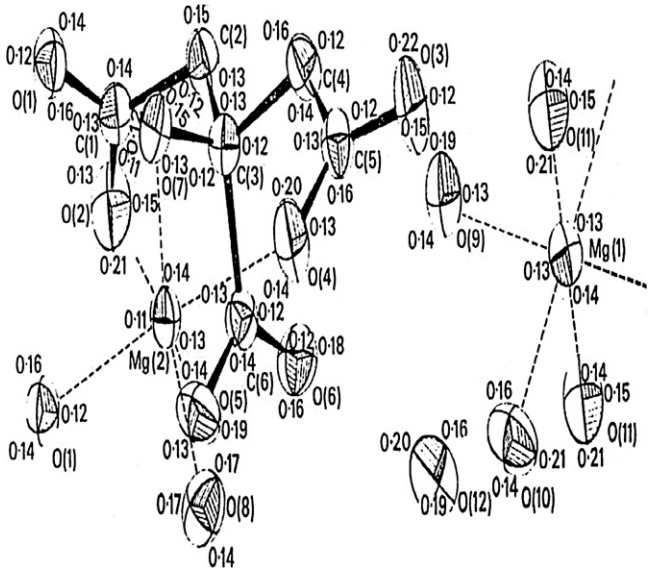

Fig. 4. The citrate ion and two Mg^{2+} ions with their complete coordination environments in the structure of doped magnesium citrate decahydrate.

g tensor do not agree with any other vector of the octahedron. This is expected considering the distorted nature of the six-fold coordination around the guest ion.

In the study of Cu^{2+} ions in magnesium citrate decahydrate it is found that the electric field symmetry around Cu^{2+} ion is rhombic. The ground state wave function in such crystals has been determined by the formula $\alpha|x^2 - y^2\rangle + \beta|3x^2 - r^2\rangle$ [20], where α is very near to unity and β is very less than unity. By using the theory of Bleaney et al. [21] several workers [22,23] have studied the ground state wave function of Cu^{2+} ion in different lattices. A similar procedure has been adopted in the present study.

The ground state wave function of Cu^{2+} ion in magnesium citrate decahydrate thus obtained is

$$(0.824)|x^2 - y^2\rangle + (0.201)|3z^2 - r^2\rangle. \quad (2)$$

It is also attempted to obtain $\delta g = g_y - g_x$ as well as the spin-exchange polarization/Fermi contact parameter, K of Cu^{2+} ion which represents the admixture of configurations with s electrons caused by spin-exchange polarization. The difference between g_y and g_x (δg_{exp}) is compared with the calculated value δg_{cal}. δg is caused by the following factors:

Table 2
Direction cosines of Mg–O vectors in magnesium citrate decahydrate.

Bond	Direction cosines in a^*, b, c axis system		
	a^*	b	c
Mg (1)–O (9)	±0.3725	±0.3485	±0.8600
Mg (1)–O (10)	±0.8614	±0.5014	±0.0806
Mg (1)–O (11)	±0.4039	±0.7982	±0.4468
Mg (2)–O (1)	±0.1228	±0.7895	±0.6012
Mg (2)–O (2)	±0.0394	±0.9716	±0.2331
Mg (2)–O (4)	±0.8070	±0.0907	±0.5835
Mg (2)–O (7)	±0.5704	±0.6550	±0.4954
Mg (2)–O (8)	±0.4529	±0.5539	±0.6986

Table 3
The parameters α, β, K, P_{exp} and δg_{cal}, δg_{exp} for Cu^{2+} in magnesium citrate decahydrate.

α	β	K	$P\,(cm^{-1})$	δg^1_{cal}	δg_{exp}
0.824	0.201	0.380	0.024	0.118	0.105

(1) by mixing of the $|x^2-y^2\rangle$ orbital with the $|3z^2-r^2\rangle$ orbital. δg^1_{cal} is given by,

$$\delta g^1_{cal} = 2\sqrt{3}\beta(\Delta g_x + \Delta g_y) \quad (3)$$

(2) by the energy splitting of the $|xz\rangle$ and $|yz\rangle$ states. δg^2_{cal} is given by,

$$\delta g^2_{cal} = (1/2)\sqrt{3}\beta(\Delta g_x + \Delta g_y) \quad (4)$$

(3) by the different covalency of the $|xz\rangle$ and $|yz\rangle$ states. δg^3_{cal} is given by,

$$\delta g^3_{cal} = (1/2)\sqrt{3}(\Delta g_x + \Delta g_y)(E_1/E_2) \quad (5)$$

where E_1 is the energy difference of the $|x^2-y^2\rangle$ and $|3z^2-r^2\rangle$ states, $E_2 = E_{dt} - E_{p\pi}$, E_{dt} = energy level of a single dt electron on the Cu^{2+} ion, $E_{p\pi}$ = energy level of a single pπ electron on the attached ligand ion.

(4) by mixing of the $|yz\rangle$ orbital with the $|xy\rangle$ orbital of the first excited state. δg^4_{cal} has the same effect as in (3).

One can consider the contribution (1) first and if $\delta g^1_{cal} \neq \delta g_{exp}$, contributions (2) and (3) must be taken into account. In the present crystal $\delta g^1_{cal} = 0.118$, $\delta g_{exp} = 0.105$, indicating a good agreement between them. Thus, there is no need of adding the contributions (2) and (3) above [21]. The parameter P represents [24] the dipole–dipole interaction of the electronic and nuclear moments ($P = g_e g_N \beta\beta_N \langle r^{-3}\rangle$). The measured value of P, P_{exp} can be obtained by multiplying P_{fi} (fi = free ion, $P_{fi} = 0.036\,cm^{-1}$ for copper) by the probability of the electrons actually being in the ^2D state around Cu^{2+} ion, i.e.

$$P_{exp} = \alpha^2 P_{fi} \quad (6)$$

The parameters α, β, K, P_{exp} and δg_{cal}, δg_{exp} for Cu^{2+} ion are given in Table 3.

5. Optical spectrum

The optical absorption spectrum of Cu^{2+} ions in MCD crystal, in the wavelength range 195–1100 nm at room temperature is exhibited in Fig. 5(a) and (b). There are four strong bands in the visible region, occurring at $\nu_1 = 800.5$ nm, $\nu_2 = 712.4$ nm, $\nu_3 = 492.3$ nm and $\nu_4 = 360.2$ nm as well as seven weak bands at 567.1, 606.8, 642.0, 686.0, 866.6, 923.8 and 1069.1 nm and four bands in the ultraviolet (UV) region (two strong and two weak in intensity) occurring at about $\nu_5 = 319.8$ nm, $\nu_6 = 286.5$ nm, $\nu_7 = 220.1$ nm and $\nu_8 = 200.1$ nm. From the nature of the absorption spectrum in the visible region, the observed bands at ν_2 and ν_3 can be regarded, respectively, as the d–d transfer bands between the ground state $d_{x^2-y^2}$ and the excited states d_{xz} and d_{yz}, into which the two-fold degenerate level $d_{xz,yz}$ is split by the crystal field and spin-orbit coupling. Thus, the band at 582.3 nm (17173 cm^{-1}) which is equal to the average value of the main band ν_3 and ν_2 can be assigned as the d–d transfer band $d_{xz,yz} \leftrightarrow d_{x^2-y^2}$, being usually the most intense [25] band. The other two bands, observed at ν_1 and ν_4 are assigned as $d_{xy} \leftrightarrow d_{x^2-y^2}$ and $d_{3z^2-r^2} \leftrightarrow d_{x^2-y^2}$ transfer bands, respectively. The bands at 866.6, 923.8 and 1069.1 nm may be infrared spectral overtone and/or combination bands [26,27].

These optical data can be used to calculate the crystal field and tetragonal parameters D_q, D_s and D_t of the Cu^{2+} complexes

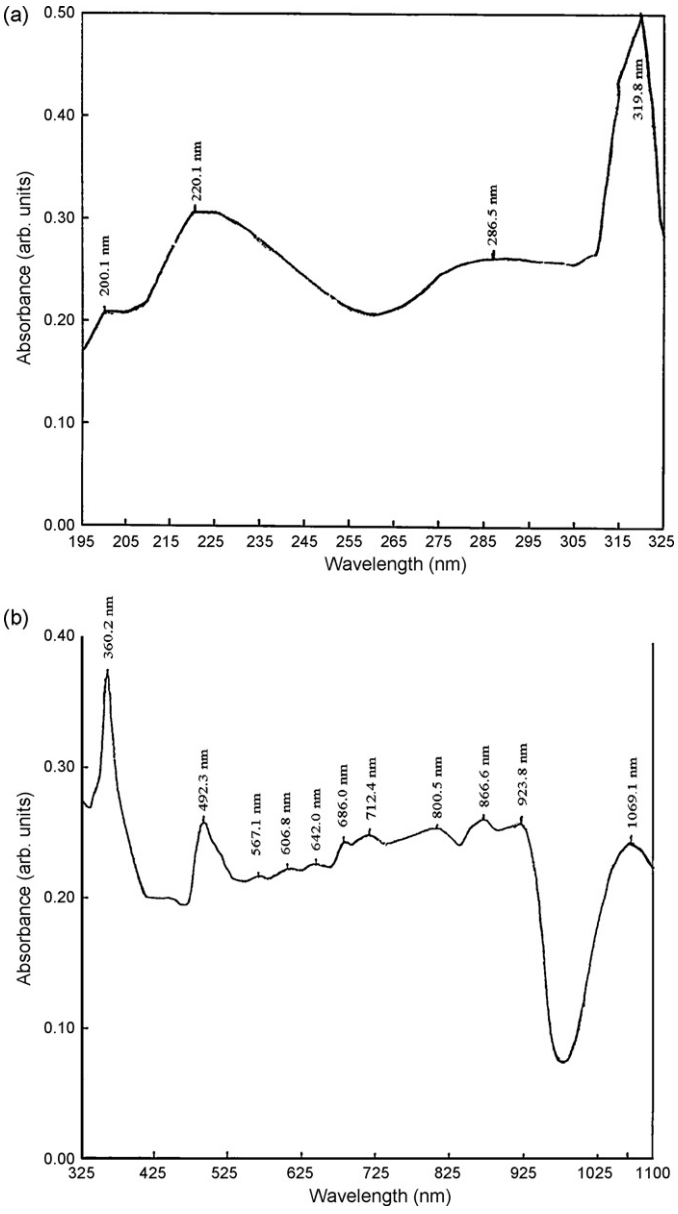

Fig. 5. (a) Optical absorption spectrum of Cu^{2+} ion doped in magnesium citrate decahydrate in wavelength range 195–325 nm. (b) Optical absorption spectrum of Cu^{2+} ion doped in magnesium citrate decahydrate in wavelength range 325–1100 nm.

from the relation given by Ballhausen and Gray [28]. The calculated parameters are $D_q = -1249.1\,cm^{-1}$, $D_s = -4634.6\,cm^{-1}$ and $D_t = -1844.3\,cm^{-1}$. These values suggest that the crystal field of the Cu^{2+} complexes under consideration is rather highly distorted tetragonal. Both the experimental energies and calculated ones using above values of D_q, D_s and D_t [29] of d–d transfer bands are given in Table 4.

Table 4
Observed and calculated energies, and assignments of the bands for Cu^{2+} in magnesium citrate decahydrate.

Transition	Band positions (nm)	
	Calculated	Observed
$d_{xy} \leftrightarrow d_{x^2-y^2}$	805.6	$\nu_1 = 800.5$ nm
$d_{xz,yz} \leftrightarrow d_{x^2-y^2}$	593.9	$\nu_2 = 712.4$ nm
	568.5	$\nu_3 = 492.3$ nm
$d_{3z^2-r^2} \leftrightarrow d_{x^2-y^2}$	360.2	$\nu_4 = 360.2$ nm

Table 5
MO coefficients for Cu^{2+} in magnesium citrate decahydrate.

α_0^2	β_1^2	β_0^2	β'^2	K
0.76	0.94	1.0	0.70	0.33

The four observed absorption bands in the UV region, occurring at $\nu_5 = 319.8$ nm, $\nu_6 = 286.5$ nm, $\nu_7 = 220.1$ nm and $\nu_8 = 200.1$ nm are, probably, charge-transfer transition bands, because they arise from the higher lying energy levels. The present results can be compared with those for $CuCl_4^{2-}$ complex [30] for which there have been observed four charge-transfer transitions in the UV range, they have been assigned as $1a_{2g} \leftrightarrow 3b_{1g}$, $4e_u \leftrightarrow 3b_{1g}$, $3e_u \leftrightarrow 3b_{1g}$ and $2a_{1g} \leftrightarrow 3b_{1g}$ transitions, in order of decreasing wavelengths. Using these results for $CuCl_4^{2-}$ the four transitions $1a_{2g} \leftrightarrow 3b_{1g}$, $4e_u \leftrightarrow 3b_{1g}$, $3e_u \leftrightarrow 3b_{1g}$ and $2a_{1g} \leftrightarrow 3b_{1g}$ correspond to the observed frequencies $\nu_5 = 319.8$ nm, $\nu_6 = 286.5$ nm, $\nu_7 = 220.1$ nm and $\nu_8 = 200.1$ nm.

6. MO analysis of the EPR data

It can be seen from Table 1 that $g_z > g_y > g_x$. When the ratio of $R = (g_y - g_x)/(g_z - g_y)$ is less than unity, the unpaired electron is predominantly in the $d_{x^2-y^2}$ state and when R is greater than unity, the unpaired electron is in $d_{3z^2-r^2}$ state [31]. The value of R for the present Cu^{2+} complex is 0.43 (less than unity), so the ground state of the electron is predominantly $d_{x^2-y^2}$. In fact, when the site symmetry is rhombic or lower, the ground state will be neither $d_{x^2-y^2}$ nor $d_{3z^2-r^2}$ but an admixture of both [32–35]. The distortion can be accounted for more clearly by the ground state wave function of the Cu^{2+} ion.

Assuming overlap integrals to be zero and omitting the small terms in the general expressions for the spin Hamiltonian parameters [36], we have

$$g_z = 2.0023 - \frac{8\alpha_0^2\beta_1^2\lambda_0}{E_{xy}} \quad (7)$$

$$g_y = 2.0023 - \frac{2\alpha_0^2\beta_0^2\lambda_0}{E_{xz}} \quad (8)$$

$$g_x = 2.0023 - \frac{2\alpha_0^2\beta'^2\lambda_0}{E_{yz}} \quad (9)$$

$$\frac{A_z}{P_0} = \left(-K - \frac{4}{7}\right)\alpha_0^2 + \Delta g_z + \left(\frac{3}{14}\right)\Delta g_y + \left(\frac{3}{14}\right)\Delta g_x \quad (10)$$

$$\frac{A_y}{P_0} = \left(-K + \frac{2}{7}\right)\alpha_0^2 + \Delta g_y - \left(\frac{3}{14}\right)\Delta g_x \quad (11)$$

$$\frac{A_x}{P_0} = \left(-K + \frac{2}{7}\right)\alpha_0^2 + \Delta g_x - \left(\frac{3}{14}\right)\Delta g_y \quad (12)$$

where $\lambda_0 = -829\,cm^{-1}$, $P_0 = 0.036\,cm^{-1}$, $\Delta g_i = g_i - 2.0023$ [36]. The α_0^2 and Fermi contact parameter K can be calculated from equations

$$\alpha_0^2 = \frac{7}{12}\left[\left(\frac{A_x + A_y - 2A_z}{P_0}\right) + 2\Delta g_z - \left(\frac{5}{14}\right)(\Delta g_x + \Delta g_y)\right] \quad (13)$$

$$K = \frac{1}{\alpha_0^2}\left[-\frac{A_z}{P_0} - \left(\frac{4}{7}\right)\alpha_0^2 + \Delta g_z + \left(\frac{3}{14}\right)(\Delta g_x + \Delta g_y)\right] \quad (14)$$

Using different permutations of the signs of A_x, A_y and A_z, we have found that only $A_x > 0$, $A_y > 0$ and $A_z < 0$ give the acceptable value of α_0^2. Taking observed values of E_{yz}, E_{xz} and E_{xy}, the estimated MO coefficients are given in Table 5.

The value of α_0^2 indicates that the σ-bonding is partly covalent in nature. β_1^2 and β_0^2 indicate that in-plane and out-of-plane π-bonding is weaker. The $\beta_0^2 = 1$ and $\beta'^2 = 0.70$ indicate that there is a ligand atom located close to apical positions of the Cu (II) complex.

The parameter K is a measure of the polarization produced by the uneven distribution of d-electron density on the inner core s-electrons and it has been suggested [37] that for 3d transition metal ions $K \approx 0.3$. The value of K obtained here is consistent with this.

Moderate π-bonding in Cu^{2+}:MCD indicates that it can be used as non-linear optical material [13]. The absorption band at 492.3 nm suggests that there can be emission of green radiation using appropriate laser and thus the second harmonic generation [38]. This supports the statement regarding the use of the present crystal as non-linear optical material. Further studies to confirm the non-linear optical properties of Cu^{2+}:MCD crystals are in progress and will be published soon.

7. Conclusion

EPR and optical absorption study of Cu^{2+} an ion in magnesium citrate decahydrate has been done at room temperature. The principal g and A parameters are evaluated from EPR spectra and are fitted to rhombic symmetry spin Hamiltonian. The angular variation plot showed that the Cu^{2+} ion enters the lattice substitutionally in place of one of the two magnesium sites, Mg (2). The ground state wave function for Cu^{2+} in the lattice has been constructed. The g-anisotropy, Fermi contact and molecular orbital parameters have been determined. Optical spectra have been explained taking into account the spin–orbit coupling. The MO coefficients indicate that the σ-bonding is partly covalent whereas in-plane and out-of-plane π-bonding is moderate. Moderate π-bonding and absorption band at 492.3 nm in Cu^{2+}:MCD suggest that it can be used as non-linear optical material.

Acknowledgement

The authors are thankful to Dr. T.K. Gundu Rao, SAIF, I.I.T. Powai, Mumbai, for providing the facility of EPR spectrometer. One of the authors, Prashant Dwivedi, is thankful to the Head of Physics Department, University of Allahabad, Allahabad for providing departmental facilities.

References

[1] W. Sano, E.D. Mauro, J. Phys. Chem. Solids 58 (1997) 391.
[2] F. Koksal, I. Kartal, B. Karabulut, Z. Naturforsch. A 54 (1999) 177.
[3] R. Tapramaz, B. Karabulut, F. Koksal, J. Phys. Chem. Solids 61 (2000) 1367.
[4] V.K. Jain, V. Kapoor, Acta Phys. Polon. A 82 (1992) 579.
[5] K.B. Narsimhalu, C.S. Sunandana, J. Lakshman Rao, Phys. Stat. Sol. B 217 (2000) 991.
[6] R. Kripal, S. Mishra, J. Magn. Magn. Mater. 294 (2005) 72.
[7] M.B. Massa, S.D. Dalosto, M.G. Ferreyra, G. Labadie, R. Calvo, J. Phys. Chem. A 103 (1999) 2606.
[8] B. Lonerdal, A.C. Stanislowski, L.S. Hurley, J. Inorg. Biochem. 12 (1980) 71.
[9] R. Swanson, W.H. Ilsley, A.C. Stanislowski, J. Inorg. Biochem. 18 (1983) 187;
N. Wu, W.F. Thon, H. Krah, R. Schlick, U. Jonas, World J. Urol. 12 (1994) 323.
[10] S. Vradelis, E. Kalaitzakis, Y. Sharifi, O. Buchel, S. Keshav, R.W. Chapman, B. Braden, World J. Gastroentol. 15 (2009) 1759 (http://www.cancer.org/docroot/CDG/content/CDG_magnesium_citrate.asp).
[11] L.T. Iseri, Am. J. Cardiol. 65 (1990) 45K (http://www.drugs.com/mtm/magnesium-citrate.html).
[12] G.A. Quamme, Am. J. Physiol. 256 (1989) 197;
J.S. Lindberg, M.M. Zobitz, J.R. Poindexter, C.Y.C. Pak, J. Am. Coll. Nutr. 9 (1990) 48;
C. Coudray, M. Rambeau, C. Feillet-Coudray, E. Gueux, J.C. Tressol, A. Mazur, Y. Rayssiguier, Magnesium Res. 18 (2005) 215 (http://astronutrition.com/magnesium-citrate.html).
[13] Z.H. Sun, D. Xu, X.Q. Wang, X.J. Liu, G. Yu, G.H. Zhang, L.Y. Zhu, H.L. Fan, Cryst. Res. Technol. 42 (2007) 812.
[14] T.B. Rao, M. Venkateshwarlu, Solid State Commun. 44 (1982) 1617.
[15] M. Venkateshwarlu, T.B. Rao, A. Hussain, Solid State Commun. 78 (1991) 1073.
[16] C.K. Johnson, Acta Cryst. 18 (1965) 1004.
[17] D.S. Schonland, Proc. Phys. Soc. 73 (1958) 788;
J.R. Pilbrow, Transition Ion EPR, Clarendon Press, Oxford, 1990.
[18] M. Korkmaz, B. Aktas, J. Phys. Chem. Solids 44 (1983) 651.
[19] M. Korkmaz, O. Korkmaz, S. Kospancali, Phys. Stat. Sol. B 112 (1982) 423.
[20] B.N. Misra, R. Kripal, Chem. Phys. 19 (1977) 17.
[21] B. Bleaney, K.D. Bowers, M.H.L. Pryce, Proc. R. Soc. A 228 (1955) 166.

[22] Z. Sroubek, K. Zdansky, J. Chem. Phys. 44 (1966) 3078;
S.K. Misra, C. Wang, J. Phys.: Condens. Matter 1 (1989) 771.
[23] B.A. Sastry, G.S. Sastry, Indian J. Pure Appl. Phys. 12 (1974) 748;
R.M. Krishna, J.L. Rao, V.V. Bhaskar, S.V.J. Lakshman, Phys. Stat. Sol. B 171 (1992) 227.
[24] T.F. Yen, Electron Spin Resonance of Metal Complexes, Plenum Press, New York, 1969, p. 153;
G. Jayaram, V.G. Krishnan, Phys. Rev. B 49 (1994) 271.
[25] D.W. Smith, J. Chem. Soc. A (1970) 176.
[26] D.E. Billing, B.J. Hathaway, P. Nicholls, J. Chem. Soc. A (1970) 1877;
B.J. Hathaway, D.E. Billing, Coord. Chem. Rev. 5 (1970) 143.
[27] R. Kripal, D.K. Singh, J. Phys. Chem. Solids 67 (2006) 2559.
[28] C.J. Ballhausen, H.B. Gray, Inorg. Chem. 1 (1962) 111.
[29] J. Ferguson, Prog. Inorg. Chem. 12 (1970) 159;
S.K. Misra, C. Wang, Phys. Stat. Sol. B 154 (1989) 259.
[30] S.D. Desjardins, K.W. Penfield, S.L. Cohen, R.L. Musselman, E.I. Soloman, J. Am. Chem. Soc. 105 (1983) 4590.
[31] A.A. Alybakov, V.A. Gubanova, K. Kudabaev, K. Sharsheev, Phys. Stat. Sol. B 146 (1988) K135.
[32] M.C.M. O'Brien, Proc. Roy. Soc. A 281 (1964) 323.
[33] Z. Sroubek, K. Zdansky, E. Simanek, Phys. Stat. Sol. 6 (1964) K149.
[34] T. Bhaskar Rao, M. Narayana, Phys. Stat. Sol. B 106 (1981) 601.
[35] P. Chand, G.C. Upreti, M. Umar, R.J. Singh, Phys. Stat. Sol. B 131 (1985) 357.
[36] D. Attanasio, J. Magn. Reson. 26 (1977) 81;
S.K. Hoffmann, M.A. Augustyniak, Acta Phys. Polon. A 74 (1988) 651.
[37] J.H. Van Vleck, Phys. Rev. 41 (1932) 208;
R.E. Watson, A.J. Freeman, Hyperfine Interactions, Academic Press, N.Y, 1967, p. 65.
[38] R.B. Kannan, A. Chandramohan, J.C. Sekar, M.A. Kandhaswamy, Cryst. Res. Technol. 42 (2007) 595.